Developmental Cell
Short Article

Two Cell Lineages, *myf5* and *myf5*-Independent, Participate in Mouse Skeletal Myogenesis

Malay Haldar,[1,2] Goutam Karan,[1] Petr Tvrdik,[1] and Mario R. Capecchi[1,2,*]
[1]Department of Human Genetics
[2]Howard Hughes Medical Institute
University of Utah, Salt Lake City, UT 84112, USA
*Correspondence: mario.capecchi@genetics.utah.edu
DOI 10.1016/j.devcel.2008.01.002

SUMMARY

In skeletal muscle development, the myogenic regulatory factors *myf5* and *myoD* play redundant roles in the specification and maintenance of myoblasts, whereas *myf6* has a downstream role in differentiating myocytes and myofibers. It is not clear whether the redundancy between *myf5* and *myoD* is within the same cell lineage or between distinct lineages. Using lineage tracing and conditional cell ablation in mice, we demonstrate the existence of two distinct lineages in myogenesis: a *myf5* lineage and a *myf5*-independent lineage. Ablating the *myf5* lineage is compatible with myogenesis sustained by *myf5*-independent, *myoD*-expressing myoblasts, whereas ablation of the *myf6* lineage leads to an absence of all differentiated myofibers, although early myogenesis appears to be unaffected. We also demonstrate here the existence of a significant *myf5* lineage within ribs that has an important role in rib development, suggested by severe rib defects upon ablating the *myf5* lineage.

INTRODUCTION

Transient condensations of paraxial mesoderm, known as somites, are the major source of skeletal muscle in vertebrates. Somites differentiate into dorsolateral dermomyotome (source of skeletal muscle and dermis) and ventromedial sclerotome (source of ribs and vertebrae). Myoblasts are proliferating progenitors of the myogenic lineage that differentiate into myocytes, and several myocytes fuse to form mature multinucleated myofibers (Buckingham et al., 2003; Parker et al., 2003). Myogenesis involves complex transcriptional networks in which the basic helix-loop-helix domain containing myogenic regulatory factors (MRFs) *myf5*, *myoD*, *myf6* (*mrf4*), and *myoG* is downstream to the paired domain transcription factors *pax3* and *pax7* (Parker et al., 2003; Pownall et al., 2002).

Relatively normal myogenesis in $myf5^{-/-}$ and $myoD^{-/-}$ mice, absence of myogenesis due to loss of myoblasts in $myf5^{-/-}$ $myoD^{-/-}$ double null mice, and lack of differentiated myofibers in $myoG^{-/-}$ mice collectively suggest a genetic hierarchy in which *myf5* and *myoD* have an upstream, redundant role in specification and maintenance of myoblasts, whereas *myoG* has a downstream role in differentiating myocytes and myofibers (Braun and Arnold, 1995; Braun et al., 1992; Hasty et al., 1993; Nabeshima et al., 1993; Rudnicki et al., 1992, 1993). However, the basis of functional redundancy between *myf5* and *myoD* has been a matter of debate. Whereas the serial lineage model assumes expression of both genes within the same lineage, the parallel lineage model purports the existence of distinct lineages. Similar to *myoG*, initial knock out studies implicated *myf6* in terminal differentiation (Braun and Arnold, 1995; Patapoutian et al., 1995; Zhang et al., 1995). A subsequent study, however, showed that $myf5^{-/-}$ $myoD^{-/-}$ double mice null lacking myoblasts were also deficient in *myf6*, and restoring *myf6* expression in these mice partially rescued embryonic myogenesis, thereby calling to question the position of *myf6* in the genetic hierarchy (Kassar-Duchossoy et al., 2004).

The lateral part of the dermomyotome is thought to play a role in the development of distal rib (Hirao and Aoyama, 2004; Kato and Aoyama, 1998). Severe rib anomalies in $myf5^{-/-}$ as well as $myf6^{-/-}$ mice suggested a role for *myf5* and *myf6* in rib morphogenesis (Braun et al., 1992; Yoon et al., 1997), but their relative involvement was unclear. Rib anomalies associated with $myf6^{-/-}$ were proposed to be the result of *cis* effects of the $myf6^{-/-}$ null on the linked *myf5* locus (Kaul et al., 2000; Yoon et al., 1997). However, a conditionally generated $myf5^{-/-}$ mutant, developed subsequently, showed no rib defects, and the authors concluded that the previously documented rib anomalies were due to long-range *cis* effects of the *neo* cassette on a putative distal gene (Kaul et al., 2000). Although the above-described observations appear to rule out a direct role of the *myf5* gene itself on rib formation, the significance of the *myf5* cell lineage in rib development is not known.

In this study, we use conditional cell ablation and lineage tracing in mice to demonstrate that *myf5* is expressed in only a subset of developing myoblasts. Early ablation of *myf5*-expressing cells during embryogenesis is compatible with myogenesis, sustained by a *myf5*-independent myoblast lineage. Surprisingly, such a redundancy does not exist for the *myf5* lineage in developing ribs, and loss of this lineage leads to a severe mutant rib phenotype. We also demonstrate an expansion in the *myoD*-expressing myoblast population upon ablating *myf5*-expressing cells, suggesting remarkable adaptability of the myogenic program to developmental insults. However, ablating the genetically downstream *myf6*-expressing cells has the opposite effect of preserving normal rib morphogenesis, while eliminating differentiated myofibers, ascertaining that *myf6* plays a predominant role in differentiated cells of skeletal muscle.

RESULTS

Alleles of *myf5* and *myf6* Cre Drivers: *Cis* Effect of Selection Cassette

myf5 and *myf6* are linked genes on mouse chromosome 10. *myf5-cre* and *myf6-cre* mice (Figure 1A) were previously generated in our laboratory and harbor an *IRES-CRE-FRT-NEO-MC1-FRT* sequence in the 3′UTR of the respective genes (Haldar et al., 2007; Keller et al., 2004). Previous reports suggested the *cis* effects of the selection cassette on the linked *myf5* and *myf6* loci as a cause of rib anomalies (Kaul et al., 2000). Although *myf5-ICN* and *myf6-ICN* mice ("*ICN*" denotes *IRES-CRE-NEO-MC1*) lack any rib phenotype in the homozygous or heterozygous state, we hypothesized that the exogenous *MC1* promoter could have a local *cis* effect. *myf6-ICN* and *myf5-ICN* mice were bred to *flp-e* mice (Rodriguez et al., 2000), thereby removing the *MC1-Neo* selection cassette (Figures 1B and 1C) and generating two alleles for each of these Cre drivers: *myf5-ICN*, *myf5-NN*, *myf6-ICN*, and *myf6-NN* ("*NN*" denotes "no neo").

Semiquantitative real-time RT-PCR and reporter-based lineage analysis revealed that the presence of the selection cassette in the 3′UTR of *myf6* or *myf5* downregulates expression of the respective genes. This is demonstrated by significantly reduced *myf6* expression and by the *myf6* lineage in *myf6-ICN* heterozygous mice (Figures 1D and 1H) compared to *myf6-NN* heterozygous mice (Figures 1E and 1I). Similarly, *myf5* expression and its lineage are significantly reduced in *myf5-ICN* heterozygous mice (Figures 1F and 1J) compared to *myf5-NN* heterozygous mice (Figures 1G and 1K). The expression of the linked gene (*myf5* expression in *myf6-NN* and vice versa) was not affected in the *NN* alleles, and expression of *myf5* and *myf6* in the heterozygous *NN* alleles was comparable to wild-type (Figures 1E and 1G). This underscores the importance of selection cassette removal in developmental studies and is the justification of our use of the *NN* allele in subsequent analysis.

The Myogenic Lineage of *myf5*

myf5 is involved in myoblast specification and maintenance (Parker et al., 2003; Pownall et al., 2002). *myf5-NN* mice were bred to *ROSA-LacZ* (*R-LZ*) reporter mice (Soriano, 1999). The resulting *myf5-NN/R-LZ* embryos revealed the expected distribution of the *myf5* lineage in whole mount (Figures 2Aa–2Ac; Figures S1Aa and S1Ab; see the Supplemental Data available with this article online) and in sections (Figure 2Ad; Figures S1Ac and S1Ad). Cre-induced expression of β-galactosidase (β-gal) recapitulates the *myf5* lineage, as suggested by consistent colocalization of the Myf5 protein with β-gal on sections (Figure 2Ae).

myf5-NN mice were then bred to reporter mice conditionally expressing the nuclear-localized β-gal reporter gene from the *CAG* promoter (*nLacZ* mouse line, P.T. and M.R.C., unpublished data) to generate *myf5-NN/nLacZ* mice. Myoblasts differentiate into myocytes that fuse to form multinucleated myofibers. Therefore, if all myoblasts express *myf5*, then all myonuclei within *myf5-NN/nLacZ* should express β-gal. Surprisingly, we detected β-gal in only a fraction of adult myonuclei based on both immunohistochemistry, a more specific method (Figures 2Ba–2Bc), and enzymatic detection of β-gal activity, a more sensitive method (Figures 2Bd and 2Be). This was true for both fast-type (Figures 2Ba and 2Bb) and slow-type myofibers (Figure 2Bc). Intercostals and leg flexors of *myf5-NN/nLacZ*, used as representative musculature, were sectioned and labeled with anti-MyHC (skeletal muscle specific), anti-β-gal (*myf5* lineage marker), and DAPI (non-specific nuclear marker). The number of β-gal-positive nuclei within MyHC-positive myofibers were counted and divided by the total number of nuclei (β-gal positive and/or DAPI positive) within MyHC-expressing myofibers. Based on this strategy, ~35% of myonuclei appeared to be a lineage of *myf5* (2012 nuclei counted). Myonuclei are located peripherally, and there is a small probability of erroneously counting adjacent nonmyogenic connective tissue nuclei within the total pool of myonuclei used in the calculation. Another possible source of error could be the sensitivity of the technique. Considering these probable sources of error, we believe that the final contribution of *myf5* to adult musculature could be as high as 50%. To rule out mosaic activity of the *CAG* promoter in myonuclei of *nLacZ* reporter mice, we bred the *nLacZ* mice to *hprt-cre* mice (Tang et al., 2002), which express Cre recombinase at the single-cell zygotic stage. All myonuclei of *hprt-cre/nLacZ* mice showed β-gal, ruling out promoter mosaicism as a potential cause of the observed partial myogenic contribution of the *myf5* lineage (Figure S1B).

The *myf5* Lineage in Embryonic Myogenesis

myf5-NN mice were bred to transgenic *ZEG* reporter mice, which express green fluorescent protein (GFP) in response to Cre (Novak et al., 2000). Based on GFP and MyoD expression in E12.5 *ZEG/myf5-NN* embryos, we identified three populations of cells: cells expressing *GFP* only (*myf5* lineage not expressing *myoD*), cells expressing *myoD* only (*myoD*-expressing cells not derived from *myf5*), and cells expressing GFP and MyoD (Figure 2C; Figures S2Aa and S2Ad). This suggests the existence of *myf5*-independent (MyoD-positive, GFP-negative) and *myf5*-expressing (GFP-positive) myoblasts. Approximately 71% of the total MyoD expression in the epaxial region (Figure 2C, left, blue boxes) and 57% in the hypaxial region (Figure 2C, right, gray boxes) occurred within the *myf5* lineage, suggesting either a predominant role or an earlier appearance of the *myf5* lineage in the epaxial compared to the hypaxial region. Approximately 32% of the *myf5* lineage showed MyoD expression in the epaxial region, and 39% showed expression in the hypaxial region (Figure 2C), suggesting the presence of either nonmyogenic *myf5* lineages or MyoD-negative myoblasts. Most of the MyoD-negative *myf5* lineages are located superficially in the epaxial domain (Figure S2Aa, arrow), are negative for MyHC (Figure S2Ab, arrow), and probably represent nonmyogenic dermal precursors (Hadchouel et al., 2000). Differentiating myocytes expressing MyHC (Figures S2Ab and S2Ae) and MyoG (Figures S2Ac and S2Af) were found within and outside the *myf5* lineage in epaxial and hypaxial regions, suggesting that both the *myf5* and *myf5*-independent lineages contribute to embryonic musculature. Moreover, Myf5 and MyoD proteins do not always colocalize at various embryonic stages (Figure S2B), further supporting the notion of distinct myoblast lineages.

The *myf5* Lineage Is Dispensable in Myogenesis

Our results suggested that all myonuclei are not derived from *myf5*-expressing cells. We then asked if the *myf5* lineage is

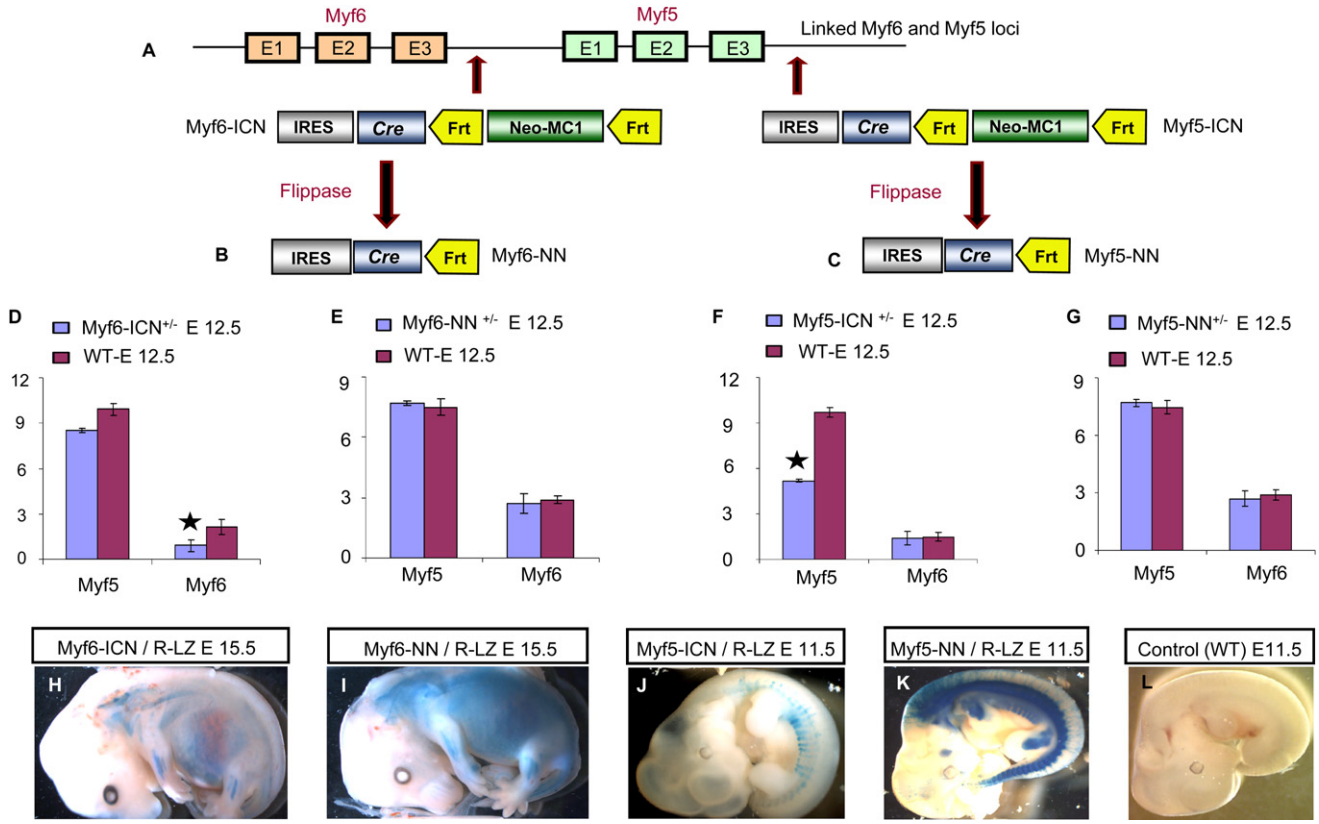

Figure 1. Alleles of *myf5* and *myf6* Cre Drivers

(A) *myf5* and *myf6* genes are linked on chromosome 10. The 3′UTR of *myf6* (in *myf6-ICN*) or *myf5* (in *myf5-ICN*) harbors an encephalomyocarditis Internal Ribosomal Entry Site (IRES) that is linked to the Cre coding sequence and is followed by the Neomycin (*neo*)-resistance selection cassette with *MC1* promoter. The selection cassette with *MC1* promoter is flanked by two *FRT* sequences.

(B and C) Breeding with *FLP-e* mice leads to recombination between *FRT* sites, generating the "*NN*" alleles.

(D–G) Semiquantitative RT-PCR on total RNA from E12.5 embryos shows (D) reduced expression of *myf6* in *myf6-ICN*$^{+/-}$ mice (star) but (E) normal expression in *myf6-NN*$^{+/-}$ mice compared to wild-type. Similarly, *myf5* expression is (F) reduced in *myf5-ICN*$^{+/-}$ mice (star) but (G) normal in *myf5-NN*$^{+/-}$ mice compared to wild-type.

(H and I) β-gal staining revealed a reduced *myf6* lineage in E15.5 (H) *myf6-ICN/R-LZ* embryos compared to (I) *myf6-NN/R-LZ* embryos.

(J and K) Similarly, the *myf5* lineage in E11.5 (J) *myf5-ICN/R-LZ* embryos is reduced compared to (K) *myf5-NN/R-LZ* embryos.

(L) A control wild-type E11.5 embryo shows an absence of any β-gal staining.

required for myogenesis. *myf5-NN* mice were bred to *ROSA-DTA* (*R-DTA*) mice conditionally expressing the highly potent diphtheria toxin (*DTA*) from the *ROSA* locus (Wu et al., 2006). Surprisingly, despite ablating the *myf5* lineage, myogenesis was preserved, as demonstrated by the presence of myofibers of both the fast type (Figure 2Da) and the slow type (Figure 2Db). Muscles were present in all anatomical regions surveyed (Figures S3Aa–S3Ad), and myofibers had normal morphology on sections (Figure 2Dc). However, these pups do not survive after birth due to a fatal rib anomaly (discussed later). The functional integrity of the musculature was demonstrated by spontaneous and stimulus-induced mobility in *myf5-NN/R-DTA* full-term embryos delivered by C-section, whereas ultrastructural integrity was demonstrated by electron microscopy (Figure 2Dd). It is noteworthy that whereas the *myf5-NN/R-DTA* mice die perinatally with severe rib cage defects, 90% of the *myf5-ICN/R-DTA* mice are viable, with a normal life span, and their musculature appears to be similar to that of *myf5-NN/R-DTA* mice based on histology (Figures S3Ba and S3Bb). Subtle downregulation of *myf5* in *myf5-NN* mice (similar to the *ICN* allele), which is undetectable in the heterozygous state (analyzed in Figures 1G and 1K), may allow a small fraction of myoblasts to survive and proliferate to form musculature. This, however, seems unlikely since Myf5 expression in *myf5-NN* is unperturbed in even the homozygous state (Figure S3C).

Inefficient killing by DTA could account for ongoing myogenesis in *myf5-NN/R-DTA* mice. To rule this out, we generated *ZEG/myf5-NN/R-DTA* embryos and observed the absence of the fluorescent *myf5* lineage within these embryos (Figures 2Ee and 2Ef) compared to *ZEG/myf5-NN* (Figures 2Ea and 2Eb) embryos at E12.5. In sections, occasional cells expressing GFP (the *myf5* lineage) are observed very rarely within *ZEG/myf5-NN/R-DTA* embryos (Figures 2Eg and 2Eh), a frequency that is almost negligible when compared to littermate *ZEG/myf5-NN* embryos (Figures 2Ec and 2Ed); this finding reflects the interval between Myf5 expression and DTA-mediated cell death, which is ~12–24 hr (Wu et al., 2006). Further investigation into DTA-mediated *myf5* lineage ablation revealed that, although the *myf5* lineage is absent

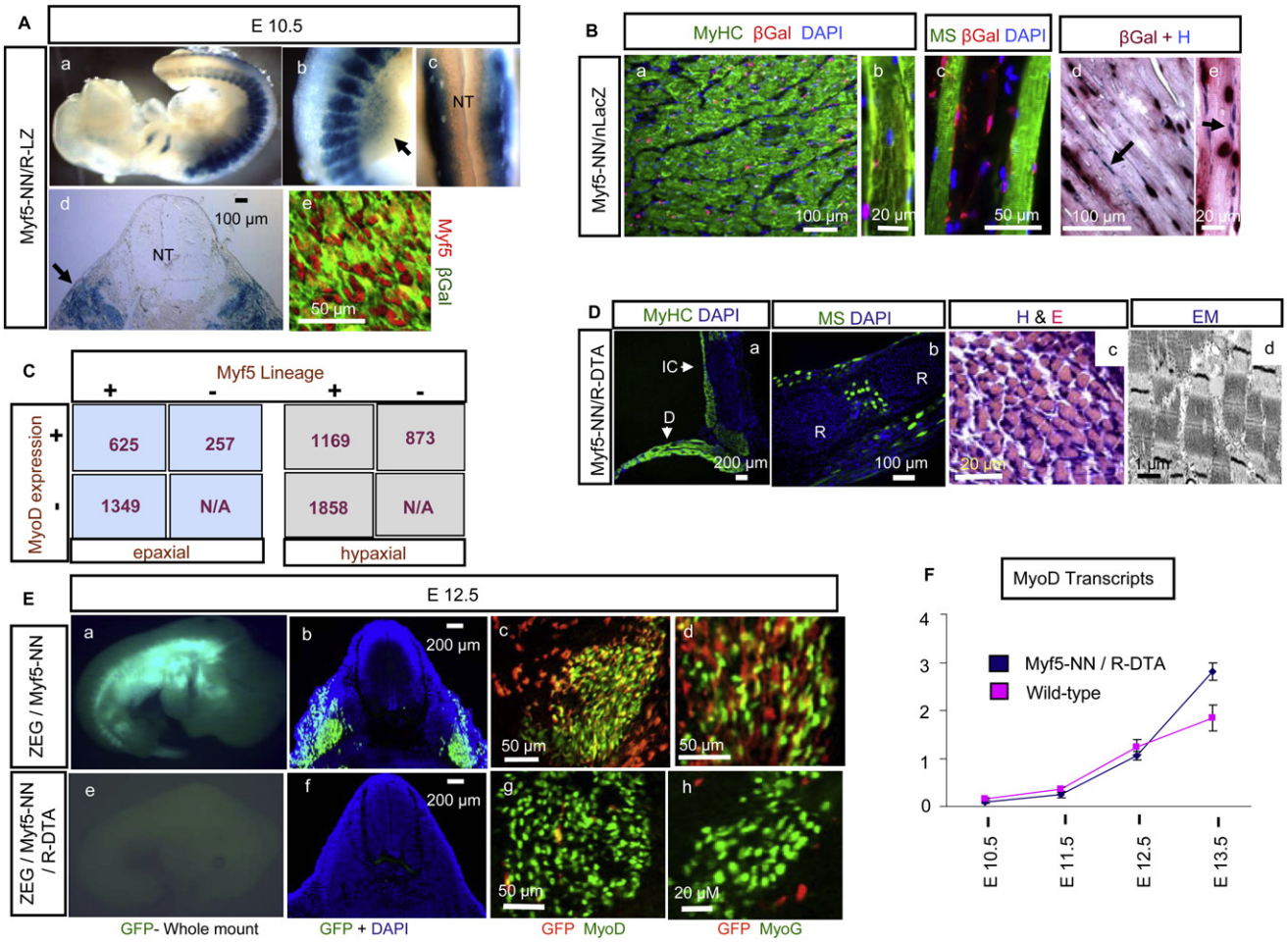

Figure 2. The *myf5* Lineage in Myogenesis

(A) (Aa) The *myf5* lineage (blue) in *myf5-NN/R-LZ* embryos comprises developing embryonic musculature at E10.5, which is predominantly in the (Ab and Ad) myotome but absent in the (Ac and Ad) neural tube. Migratory myogenic populations in the (Ab) limbs (arrow) and (Ad) nonmyogenic dermal precursors (arrows) are shown. (Ae) *myf5* expression (red, anti-Myf5) occurs exclusively within the β-gal lineage marker (green, anti-β-gal) in *myf5-NN/R-LZ* embryos.

(B) The *myf5* lineage (red, anti-β-gal) is present within (Ba and Bb) fast-type (green, anti-MyHC) myofibers and (Bc) slow-type (green, anti-MS) myofibers of adult *myf5-NN/nLacZ* intercostal muscle. (Bd and Be) Enzymatic detection of β-gal activity (red nuclei) reveals a similar distribution of the *myf5* lineage, with hematoxylin as counterstain (blue nuclei). Arrows show myonuclei not derived from Myf5.

(C) The distribution of the *myf5* lineage (with anti-β-gal) and MyoD expression (using anti-MyoD) was analyzed in epaxial (left, blue box) and hypaxial (right, gray box) regions by cell counting in E12.5 *ZEG/myf5-NN* embryos. The numbers in boxes are the numbers of nuclei counted. +, presence; −, absence.

(D) (Da) Fast-type (green, anti-MyHC) and (Db) slow-type (green, anti-MS) fibers seen in E18.5 *myf5-NN/R-DTA* intercostal musculature (D, diaphragm; IC, intercostals; R, ribs) that show normal morphology based on (Dc) H&E staining and (Dd) electron micrograph.

(E) The *myf5* lineage (green) demonstrated in (Ea) whole mount and (Eb) sections (green, anti-GFP) in E12.5 *ZEG/myf5-NN* embryos. (Ec) MyoD (gree,n anti-MyoD) and (Ed) myogenin (green, anti-MyoG) are expressed within and in proximity to the *myf5* lineage (red, anti-GFP). Absence of the *myf5* lineage in *ZEG/myf5-NN/R-DTA* embryos is demonstrated in (Ee) whole mount (absence of green signal) and (Ef) sections (absence of green anti-GFP staining). (Eg) MyoD and (Eh) MyoG expression occurs independent of the *myf5* lineage in *ZEG/myf5-NN/R-DTA*.

(F) Semiquantitative RT-PCR for *myoD* at E10.5, E11.5, E12.5, and E13.5 reveals increased numbers of MyoD transcripts in *myf5-NN/R-DTA* embryos compared to wild-type by E13.5.

(Figures 2Ee and 2Ef), *myf5* transcripts (Figure S4A) and proteins (Figures S4B and S4C) that are detectable at E11.5 are greatly reduced and are dramatically reduced further with increasing embryonic age such that by E13.5 Myf5 proteins are essentially undetectable by western blot (Figure S4B) and are barely detectable based on immunohistochemistry (Figure S4C). Furthermore, a significant population of Myf5-expressing cells at E11.5 in *myf5-NN/R-DTA* mice is already undergoing apoptosis (Figure S4Ce). These results demonstrate that in vivo cell killing via DTA is associated with a time-lag between the onset of "DTA-inducing" gene expression (in this case, *myf5*) and DTA-induced apoptosis that has to be accounted for when analyzing lineage ablation by using this system.

Ongoing myogenesis within *ZEG/myf5-NN//R-DTA* embryos based on MyoD and MyoG expression (Figures 2Eg and 2Eh) suggests that embryonic myogenesis is not significantly perturbed in the absence of the *myf5* lineage. Real-time RT-PCR analysis of *myf5-NN/R-DTA* embryos between E10.5 and

E13.5 revealed significantly higher levels of *myoD* transcripts (Figure 2F) compared to wild-type by E13.5, suggesting an expansion of *myf5*-independent, *myoD*-expressing myoblasts to compensate for the loss of the *myf5* lineage. Unlike *myoD*, there is no significant difference in *myf6* expression within *myf5-NN/R-DTA* embryos at these stages (Figure S3D), suggesting that loss of the *myf5* lineage does not affect the pool of differentiating myocytes, indicating efficient compensation by *myf5*-independent lineages.

The *myf6* Lineage Is Indispensable in Myogenesis

myf6 is believed to be genetically downstream of *myf5* and to act in differentiated cells of the skeletal muscle lineage. The *myf6* lineage is detectable by E10.5 (Figures 3Aa and 3Ab) and comprises a majority of, but not all, adult myonuclei, based on enzymatic (Figure 3Ac) and antibody-based (Figure 3Ad) detection of β-gal within *myf6-NN/nLacZ* mice. Significant Myf6 expression also occurs in adult musculature (Figure 3Ae). *myf6-NN* mice were bred to *ROSA-YFP* (*R-YFP*) reporter mice (Srinivas et al., 2001), and the *myf6* lineage was found to comprise only a small fraction of cells expressing *myoD*, *myoG*, and *myHC* (Figures 3Ba–3Bc) within E14.5 *myf6-NN/R-YFP* embryos, suggesting that *myf6* makes a minor contribution in early myogenesis. However, we observed a complete lack of differentiated myofibers in the newborn *myf6-NN/R-DTA* pups that were immobile and died soon after birth. On sections, basophilic clumps of cellular debris were observed in locations of skeletal musculature (Figures 3Ca and 3Cb), suggesting that skeletal muscles were formed prior to DTA-mediated killing. Robust expression of Myf5, MyoD, and MyoG within E12.5 *myf6-NN/R-DTA* embryos suggested that the absence of the *myf6* lineage does not significantly compromise early embryonic myogenesis (Figures 3Da–3Dc).

The number of apoptotic cells within *myf6-NN/R-DTA* embryos increased with embryonic age, as more and more differentiated cells of myogenic lineage express Myf6 and consequently DTA (Figures 3Ea and 3Eb), such that by E18.5 all differentiated myofibers were either already dead (extracellular patchy staining with MyHC) or dying (positive for activated caspase-3). These observations support the existing concept that *myf6* plays a primary role in differentiated cells of the myogenic lineage and is not crucial in early myogenesis.

The *myf5* Lineage in Rib Morphogenesis

Previous studies with targeted alleles of *myf5* replaced with the β-gal reporter gene showed the presence of β-gal-expressing rib chondrocytes in null, but not in heterozygous, mice, leading the authors to suggest that the absence of *myf5* leads to misincorporation of the *myf5* lineage in ribs (Tajbakhsh et al., 1996). We observed significant *myf5* lineage within ribs of both *myf5-NN/R-LZ* (Figures 4Aa, 4Ab, 4Ae, and 4Af) and *myf5-ICN/R-LZ* mice (Figures 4Ag and 4Ah), which comprised mostly chondrocytes and some cells in perichondrium (Figure 4Ab). The costochondral (Figures 4Af and 4Ah, arrows) and costosternal (Figures 4Ae and 4Ag, arrows) regions of ribs were particularly rich in the *myf5* lineage and appeared smaller in *myf5-ICN/R-LZ* (Figure 4Ah, arrow) compared to *myf5-NN/R-LZ* mice (Figure 4Af, arrow) at the costochondral region. This apparent quantitative difference in the rib lineage of *myf5* within the two alleles of *myf5-cre* mice (*myf5-NN* and *myf5-ICN*) translates into striking differences in the rib phenotype when these mice are bred to *R-DTA* mice. Whereas *myf5-NN/R-DTA* newborn pups have severely deformed ribs (Figures 4Ba–4Bc) and die immediately after birth, apparently due to their inability to breathe, *myf5-ICN/R-DTA* mice show normal rib cages, with few mild anomalies such as occasional waviness of floating ribs (Figures 4Ca–4Cc). The cartilaginous portion of the ribs shows fusions (Figure 4Ba, arrow) and loss of symmetric bilateral attachment to the sternum (Figure 4Bb, arrow), and the osseous portion shows occasional "knob-like" protrusions (Figure 4Bc, arrows) in the *myf5-NN/R-DTA* mice. These anomalies are detectable even at early embryonic stages, whereas heterozygous *myf5-NN* or *R-DTA* control mice show normal rib cages (Figures S5a–S5d).

The rib defects seen upon *myf5* lineage ablation could be due to extensive structural damage to developing somites. If this were true, then ablation of other somitic myotomal lineages, such as that of *pax3* or *pax7*, should recapitulate the rib phenotype of *myf5-NN/R-DTA*. Whereas *pax3-cre/R-DTA* mice suffer extensive disruption of development not compatible with embryogenesis (data not shown), *pax7-cre/R-DTA* newborn pups show no rib cage anomalies (Figures 4Da–4Dc), and *pax7* lineages were absent from ribs (Figure 4Dd). This indicates that nonspecific somitic damage is probably not the cause of rib anomalies upon *myf5* lineage ablation. Intercostal musculature of *myf5-NN/R-DTA* mice appears to be normal based on histology and electron microscopy. Moreover, ablation of the *myf6* lineage, which is absent in ribs (Figure 4Ed), eliminates all intercostal musculature while preserving rib development (Figures 4Ea–4Ec). These findings seem to rule out abnormal intercostal musculature as a cause of rib mispatterning in the absence of the *myf5* lineage. Therefore, the *myf5* lineage appears to play a direct role in rib development. Furthermore, electron microscopy of the mispatterned ribs of *myf5-NN/R-DTA* shows no obvious ultrastructural anomalies, suggesting the absence of any primary chondrocyte defect (Figures S5e and S5f).

DISCUSSION

Targeted loss-of-function analyses in mice demonstrated functional redundancy between *myf5* and *myoD* in the specification and maintenance of myoblasts. However, it was not clear whether the redundancy is within the same cell lineage (serial lineage model) or between distinct lineages (parallel lineage model). One study attempted to address this in vitro by showing that ablation of either *myf5*- or *myoD*-expressing embryonic stem cells did not compromise their myogenic line of differentiation in culture (Braun and Arnold, 1996), whereas another study suggested distinct roles of *myf5* and *myoD* in epaxial and hypaxial musculature, respectively (Kablar et al., 1997), raising the possibility of multiple myogenic lineages. Here, we demonstrate the existence of two distinct myogenic lineages: a *myf5* lineage and a *myf5*-independent lineage (MyoD expressing), which seem to be the basis of functional redundancy between *myf5* and *myoD*. The presence of such intercellular redundancy in terms of lineage commitment during embryogenesis reflects the evolution of the myogenic pathway and provides for an inbuilt safeguard against potential disruption of the myogenic program.

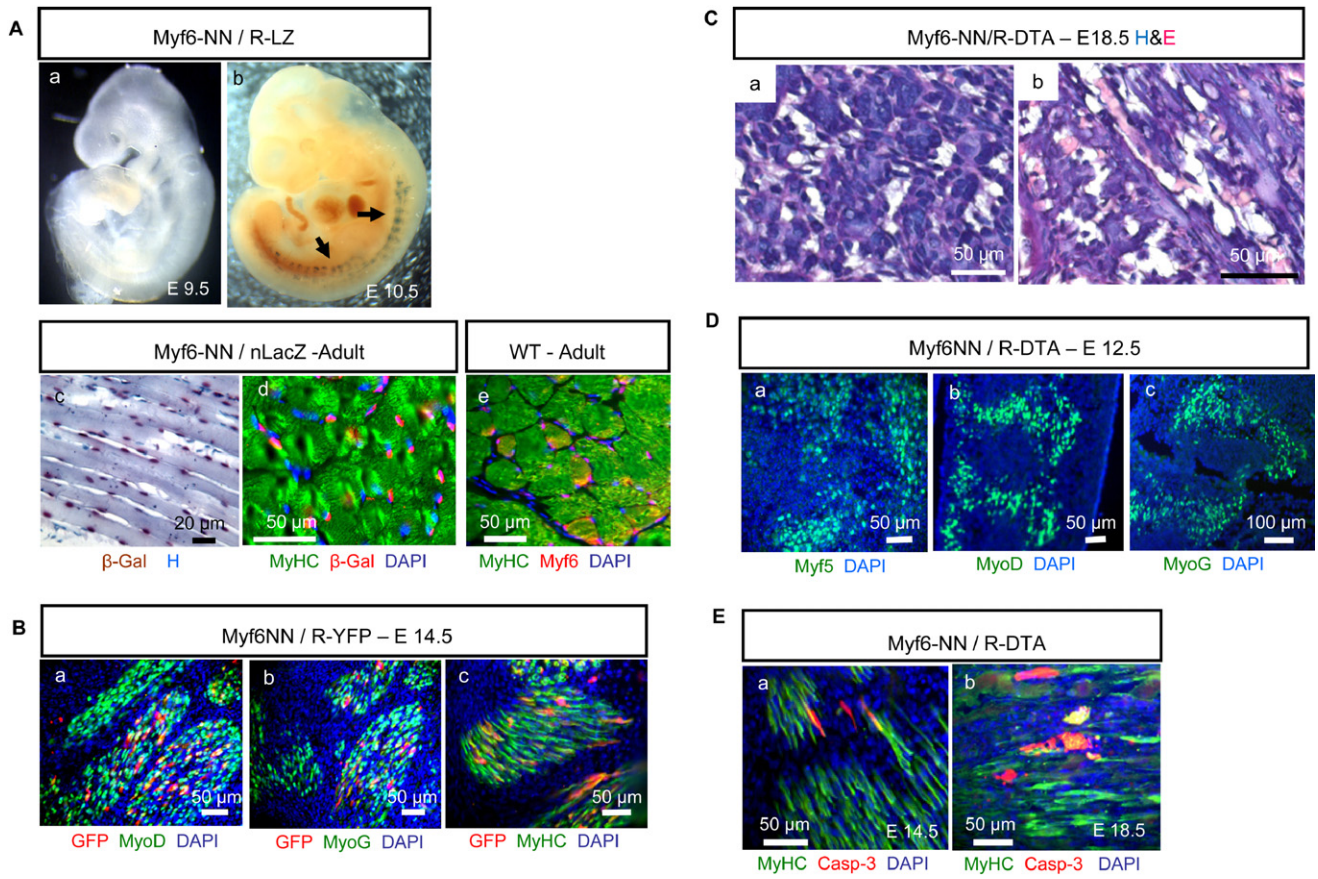

Figure 3. The *myf6* Lineage in Myogenesis

(A) *The myf6* lineage is undetectable at (Aa) E9.5 and is detectable at (Ab) E10.5 (arrows) based on β-gal staining (blue) of *myf6-NN/R-LZ* embryos. (Ac) The *myf6* lineage (red nuclei) in the intercostal musculature of an adult *myf6-NN/nLacZ* mouse is detected by β-gal staining and hematoxylin counterstain (blue nuclei). (Ad) shows the same based on immunohistochemistry (red, anti-β-gal; green, anti-MyHC). (Ae) shows Myf6 expression (red, anti-Myf6) in adult intercostal muscles (green, anti-MyHC).

(B) Transverse sections through the epaxial region of *myf6-NN/R-YFP* embryos demonstrate that the *myf6* lineage (red, anti-GFP) comprises only a fraction of (Ba) MyoD- (green, anti-MyoD), (Bb) MyoG- (green, anti-MyoG), and (Bc) MyHC-expressing (green, anti-MyHC) cells at E14.5.

(C) (Ca and Cb) E18.5 *myf6-NN/R-DTA* embryos show basophilic cellular debris in place of musculature (back muscles).

(D) Robust myogenesis within an E12.5 *myf6-NN/R-DTA* embryo demonstrated by expression of (Da) *myf5* (green, anti-Myf5), (Db) *myoD* (green, anti-MyoD), and (Dc) *myoG* (green, anti-MyoG) in sections through the myotome.

(E) Apoptosis detected by expression of activated caspase-3 (red) within differentiated myofibers (green) at (Ea) E14.5 and (Eb) E18.5.

Myf5 and MyoD expression are not mutually exclusive, as suggested by widespread expression of MyoD within the *myf5* lineage, nor are they coexpressed, as suggested by mostly distinct expression of Myf5 and MyoD. This suggests that, under normal circumstances, most of the myogenic lineage of *myf5* eventually expresses MyoD, or vice versa. The presence of skeletal musculature in the absence the *myf5* lineage, however, suggests that such sequential expression is not required for myogenesis. Compared to the final contribution of the *myf5* lineage to adult myonuclei (about 50%), a higher fraction of myoblasts (71% in epaxial musculature and 57% in hypaxial musculature) comprises a lineage of *myf5* at E12.5, suggesting that MyoD may not be expressed in all myoblasts. Therefore, *myoD*-independent myoblasts may exist in a manner similar to *myf5*-independent myoblasts that we describe here. However, we may have missed a significant proportion of the MyoD expression outside the *myf5* lineage based on the reported variability of Myf5 and MyoD expression with the cell cycle (Kitzmann et al., 1998). Another possibility could be that more *myf5*-independent lineages contribute to myogenesis at later embryonic stages (after E12.5), thereby reducing the fraction of the final *myf5* lineage in the adult musculature. In either scenario, it is not certain at this time whether the *myf5*-independent compartment is a single compartment or is heterogeneous based on MRF expression.

Cells expressing *myf5* undergoe *DTA*-mediated apoptosis within *myf5-NN/R-DTA* embryos, precluding any cell-autonomous differences in the levels of *myoD* secondary to the absence of *myf5*. Therefore, an increased number of *myoD* transcripts in *myf5-NN/R-DTA* embryos reflects an increased number of *myoD*-expressing cells that probably compensate for the loss of the *myf5* lineage to restore normal myogenesis. It would be interesting to know how the myogenic program maintains a balance between these distinct lineages and

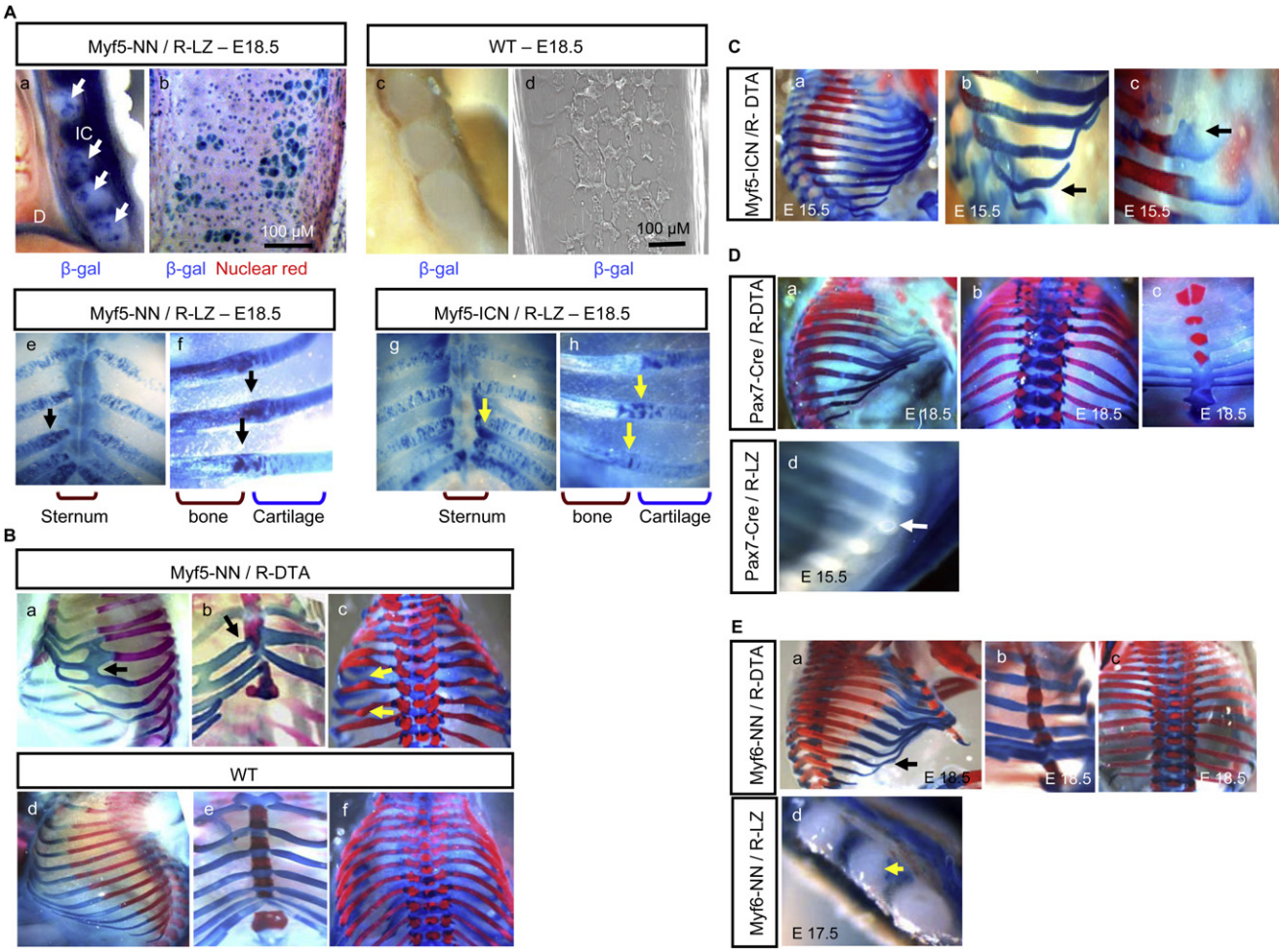

Figure 4. Unique Role of the *myf5* Lineage in Rib Morphogenesis

(A) The *myf5* lineage is detected by blue β-gal staining at E18.5 in ribs of *myf5-NN/R-LZ*, demonstrated in (Aa) whole mount (arrows) and (Ab) sections. (Aa) IC, intercostal muscles; D, diaphragm. The counterstain is nuclear red in (Ab). Control wild-type littermates show an absence of β-gal staining in (Ac) whole mount and in (Ad) sections. Rib lineages of Myf5 appear to be prominent at the (Ae and Ag) sternal end (arrows) and the (Af and Ah) costochondral region (arrows) and appear less often in the (Ah) "*ICN*" allele compared to the (Af) "*NN*" allele in costochondral regions.

(B) Abnormal rib cage of newborn *myf5-NN/R-DTA* mice characterized by (Ba) fusions (arrow) and (Bb) staggered asymmetric attachment to the sternum (arrow) at the cartilaginous part and by (Bc) abnormal protrusions in the bony part (arrow). (Bd)–(Bf) show comparative regions in a wild-type littermate.

(C) *myf5-ICN/R-DTA* mice have (Ca) normal rib cages and occasional mild anomalies such as (Cb) waviness of the floating ribs (arrow) and (Cc) occasional knobs in the costal regions (arrow).

(D) (Da–Dc) Ablating the *pax7* lineage does not perturb rib morphogenesis. (Dd) The *pax7* lineage is absent within ribs of E15.5 *pax7-cre/R-LZ* embryos (arrow).

(E) (Ea)–(Ec) Ablating the *myf6* lineage does not perturb normal rib morphogenesis, except for (Ea) occasional mild waviness (arrow). (Ed) The *myf6* lineage is absent within ribs of E17.5 *myf6-NN/R-LZ* embryos (arrow).

determines expansion or restriction of individual lineages in different scenarios. Another intriguing question is whether such distinct lineages also exist during satellite-cell-mediated postnatal myogenesis.

Skeletal muscle of *myf5-NN/R-DTA* appear to be indistinguishable from that of *myf5-ICN/R-DTA* based on histology. Therefore, *myf5-NN/R-DTA* mice, like *myf5-ICN/R-DTA* mice, would most likely have had a normal lifespan if not for the severe rib defects. It is remarkable that the lineage of *myf5*, an MRF, is dispensable in myogenesis but is required for rib development. Because a conditionally generated *myf5* null mouse that lacks rib defects has been described, it is the *myf5* cell lineage, not the *myf5* gene, that is critical for rib development, which suggests that *myf5* expression is not exclusive to the myogenic lineage. In this regard, it is noteworthy that lateral aspects of cervical vertebrae also show the presence of the *myf5* lineage (Figure S5g). Transient expression of *myf5* in presomitic mesoderm has been reported (Cossu et al., 1996), and it is possible that the presomitic cells transiently expressing *myf5* are the primary source of the substantial nonmyogenic lineages of *myf5*, whereas somitic cells initiating *myf5* expression are the primary source of *myf5*'s myogenic lineage. Whether somitic expression of *myf5* occurs within the lineages of presomitic cells that had transiently expressed *myf5* as well as the identity of the subset of *myf5*-expressing cells that are involved in rib development are currently under investigation.

In summary, we demonstrate here the existence of two independent lineages in myogenesis and show a role of the *myf5* lineage in rib development by using lineage analysis in conjunction with lineage ablation, a strategy that could be effectively applied to analyze other developmental pathways.

EXPERIMENTAL PROCEDURES

Animal Handling and Genotyping

All studies involving animal subjects were approved by the University of Utah Institutional Animal Care and Use Committee and were conducted strictly in accordance with the relevant protocol. *myf5-cre* and *myf6-cre* mouse lines have been described elsewhere (Haldar et al., 2007; Keller et al., 2004). The *nLacZ* reporter line was generated by targeting the conditional, codon-optimized, and nuclear localization signal-containing β-gal gene to the *polr2a* locus, ~1 kb downstream of the *polyA* signal. The promoter driving nLacZ expression is the *CAG* promoter, a hybrid promoter comprised of cytomegalovirus immediate early enhancer and the chicken β-actin promoter (Tang et al., 2002). The specific details of this mouse line are available upon request and will be published elsewhere.

Real-Time RT-PCR

Semiquantitative real-time RT-PCR was performed by using total RNA from wild-type and mutant embryos extracted with TRIzol (invitrogen), purified, and treated with DNase. Real-time RT-PCR was performed on RNA samples (25 ng) by using the QuantiTect SYBR green RT-PCR kit (QIAGEN, Inc., Valencia, CA) and a DNA Engine Opticon 2 system (MJ Research, Waltham, MA). Results were normalized to Gapdh signals for each sample. Standards for Gapdh and all other primer sets showed similar slopes, indicating equivalent amplification kinetics. Please refer to the Supplemental Data for primer sequences.

β-Galactosidase Staining

For whole-mount staining, samples were fixed in 1% PFA, 0.2% glutaraldehyde, 0.002 M $MgCl_2$, 0.025 M EGTA, and 0.02% NP-40 in 1× PBS for 2 hr at 4°C, followed by overnight staining at room temperature in 0.005 M $K_3Fe(CN)_6$, 0.005 M $K_4Fe(CN)_6$, 0.002 M MgCl2, 0.01% Na-doc, 0.02% NP-40, and X-gal substrate in 1× PBS. Ribs were cleared in 1% KOH/20% glycerol until soft tissues disappeared.

Fixed and cryopreserved samples were also sectioned at 8–12 μm thickness and stained at room temperature overnight in β-gal staining solution (described above). Counterstaining was carried out with hematoxylin by following the established protocol.

Whole-Mount Skeletal Staining

Skeletal staining was carried out with Alizarin red and alcian blue by following the established protocol (Wellik and Capecchi, 2003).

Histology and Immunodetection

Hematoxylin and Eosin staining was carried out on 4–8 μm sections of tissue fixed in 4% PFA and embedded in paraffin by following standard protocols. Fluorescence-based immunohistochemistry was performed on 8–12 μm fixed and frozen sections. Cell counting was carried out with help from ImageJ software by using the ITCN plug in (Byun et al., 2006).

For western blot, embryonic samples from different stages of mouse development were homogenized in 200–500 μl lysis buffer (1% Triton X-100, 0.2% SDS, .001 M EDTA in 0.05 M Tri-HCl [pH 7.4]). Each sample (15 μg protein) was separated on a 8% SDS-PAGE gel, transferred onto a PVDF gel, and probed with primary antibodies, followed by horseradish peroxidase-conjugated secondary antibody. The signal was visualized by using the chemiluminescence ECL-Plus system.

Please refer to the Supplemental Data for information on antibodies used.

Electron Microscopy

Tissue samples were fixed by using 2% formaldehyde and 2% glutaraldehyde in 0.1 M PBS (pH 7.4) containing 1% osmium tetroxide, dehydrated through an ascending series of graded ethanols, and processed for embedment in Epon 812 resin. Ultrathin sections (0.75–0.5 μm) were mounted on copper grids and stained with uranyl acetate and lead citrate before observation under an electron microscope (Philips, TECNAI-T12).

Apoptosis Detection

Apoptosis was detected by using a rabbit polyclonal antibody directed against the activated, cleaved form of caspase-3 (Cell signaling). A TUNEL assay was performed by using a fluorescein In Situ Cell Death Detection Kit (Roche), and the assay was performed according to the manufacturer's instructions.

SUPPLEMENTAL DATA

Supplemental Data include information on primer sequences and antibodies used and are available at http://www.developmentalcell.com/cgi/content/full/14/3/437/DC1/.

ACKNOWLEDGMENTS

We thank Sen Wu for generating and making available the *ROSA-DTA* mouse line, and Gabriel Kardon, Eugenio Sangiorgi, Lara Carrol, Amir Pozner, and Anne Boulet for helpful comments and insights.

Received: July 26, 2007
Revised: November 29, 2007
Accepted: January 2, 2008
Published: March 10, 2008

REFERENCES

Braun, T., and Arnold, H.H. (1995). Inactivation of *Myf-6* and *Myf-5* genes in mice leads to alterations in skeletal muscle development. EMBO J. *14*, 1176–1186.

Braun, T., and Arnold, H.H. (1996). *Myf-5* and *myoD* genes are activated in distinct mesenchymal stem cells and determine different skeletal muscle cell lineages. EMBO J. *15*, 310–318.

Braun, T., Rudnicki, M.A., Arnold, H.H., and Jaenisch, R. (1992). Targeted inactivation of the muscle regulatory gene *Myf-5* results in abnormal rib development and perinatal death. Cell *71*, 369–382.

Buckingham, M., Bajard, L., Chang, T., Daubas, P., Hadchouel, J., Meilhac, S., Montarras, D., Rocancourt, D., and Relaix, F. (2003). The formation of skeletal muscle: from somite to limb. J. Anat. *202*, 59–68.

Byun, J., Verardo, M.R., Sumengen, B., Lewis, G.P., Manjunath, B.S., and Fisher, S.K. (2006). Automated tool for the detection of cell nuclei in digital microscopic images: application to retinal images. Mol. Vis. *12*, 949–960.

Cossu, G., Tajbakhsh, S., and Buckingham, M. (1996). How is myogenesis initiated in the embryo? Trends Genet. *12*, 218–223.

Hadchouel, J., Tajbakhsh, S., Primig, M., Chang, T.H., Daubas, P., Rocancourt, D., and Buckingham, M. (2000). Modular long-range regulation of Myf5 reveals unexpected heterogeneity between skeletal muscles in the mouse embryo. Development *127*, 4455–4467.

Haldar, M., Hancock, J.D., Coffin, C.M., Lessnick, S.L., and Capecchi, M.R. (2007). A conditional mouse model of synovial sarcoma: insights into a myogenic origin. Cancer Cell *11*, 375–388.

Hasty, P., Bradley, A., Morris, J.H., Edmondson, D.G., Venuti, J.M., Olson, E.N., and Klein, W.H. (1993). Muscle deficiency and neonatal death in mice with a targeted mutation in the *myogenin* gene. Nature *364*, 501–506.

Hirao, A., and Aoyama, H. (2004). Somite development without influence of the surface ectoderm in the chick embryo: the compartments of a somite responsible for distal rib development. Dev. Growth Differ. *46*, 351–362.

Kablar, B., Krastel, K., Ying, C., Asakura, A., Tapscott, S.J., and Rudnicki, M.A. (1997). MyoD and Myf-5 differentially regulate the development of limb versus trunk skeletal muscle. Development *124*, 4729–4738.

Kassar-Duchossoy, L., Gayraud-Morel, B., Gomes, D., Rocancourt, D., Buckingham, M., Shinin, V., and Tajbakhsh, S. (2004). Mrf4 determines skeletal muscle identity in *Myf5:Myod* double-mutant mice. Nature *431*, 466–471.

Kato, N., and Aoyama, H. (1998). Dermomyotomal origin of the ribs as revealed by extirpation and transplantation experiments in chick and quail embryos. Development *125*, 3437–3443.

Kaul, A., Koster, M., Neuhaus, H., and Braun, T. (2000). Myf-5 revisited: loss of early myotome formation does not lead to a rib phenotype in homozygous *Myf-5* mutant mice. Cell *102*, 17–19.

Keller, C., Arenkiel, B.R., Coffin, C.M., El-Bardeesy, N., DePinho, R.A., and Capecchi, M.R. (2004). Alveolar rhabdomyosarcomas in conditional Pax3:Fkhr mice: cooperativity of Ink4a/ARF and Trp53 loss of function. Genes Dev. *18*, 2614–2626.

Kitzmann, M., Carnac, G., Vandromme, M., Primig, M., Lamb, N.J., and Fernandez, A. (1998). The muscle regulatory factors MyoD and myf-5 undergo distinct cell cycle-specific expression in muscle cells. J. Cell Biol. *142*, 1447–1459.

Nabeshima, Y., Hanaoka, K., Hayasaka, M., Esumi, E., Li, S., Nonaka, I., and Nabeshima, Y. (1993). *Myogenin* gene disruption results in perinatal lethality because of severe muscle defect. Nature *364*, 532–535.

Novak, A., Guo, C., Yang, W., Nagy, A., and Lobe, C.G. (2000). Z/EG, a double reporter mouse line that expresses enhanced green fluorescent protein upon Cre-mediated excision. Genesis *28*, 147–155.

Parker, M.H., Seale, P., and Rudnicki, M.A. (2003). Looking back to the embryo: defining transcriptional networks in adult myogenesis. Nat. Rev. Genet. *4*, 497–507.

Patapoutian, A., Yoon, J.K., Miner, J.H., Wang, S., Stark, K., and Wold, B. (1995). Disruption of the mouse *MRF4* gene identifies multiple waves of myogenesis in the myotome. Development *121*, 3347–3358.

Pownall, M.E., Gustafsson, M.K., and Emerson, C.P., Jr. (2002). Myogenic regulatory factors and the specification of muscle progenitors in vertebrate embryos. Annu. Rev. Cell Dev. Biol. *18*, 747–783.

Rodriguez, C.I., Buchholz, F., Galloway, J., Sequerra, R., Kasper, J., Ayala, R., Stewart, A.F., and Dymecki, S.M. (2000). High-efficiency deleter mice show that FLPe is an alternative to Cre-loxP. Nat. Genet. *25*, 139–140.

Rudnicki, M.A., Braun, T., Hinuma, S., and Jaenisch, R. (1992). Inactivation of MyoD in mice leads to up-regulation of the myogenic HLH gene *Myf-5* and results in apparently normal muscle development. Cell *71*, 383–390.

Rudnicki, M.A., Schnegelsberg, P.N., Stead, R.H., Braun, T., Arnold, H.H., and Jaenisch, R. (1993). MyoD or Myf-5 is required for the formation of skeletal muscle. Cell *75*, 1351–1359.

Soriano, P. (1999). Generalized lacZ expression with the ROSA26 Cre reporter strain. Nat. Genet. *21*, 70–71.

Srinivas, S., Watanabe, T., Lin, C.S., William, C.M., Tanabe, Y., Jessell, T.M., and Costantini, F. (2001). Cre reporter strains produced by targeted insertion of EYFP and ECFP into the ROSA26 locus. BMC Dev. Biol. *1*, 4.

Tajbakhsh, S., Rocancourt, D., and Buckingham, M. (1996). Muscle progenitor cells failing to respond to positional cues adopt non-myogenic fates in *myf-5* null mice. Nature *384*, 266–270.

Tang, S.H., Silva, F.J., Tsark, W.M., and Mann, J.R. (2002). A Cre/loxP-deleter transgenic line in mouse strain 129S1/SvImJ. Genesis *32*, 199–202.

Wellik, D.M., and Capecchi, M.R. (2003). *Hox10* and *Hox11* genes are required to globally pattern the mammalian skeleton. Science *301*, 363–367.

Wu, S., Wu, Y., and Capecchi, M.R. (2006). Motoneurons and oligodendrocytes are sequentially generated from neural stem cells but do not appear to share common lineage-restricted progenitors in vivo. Development *133*, 581–590.

Yoon, J.K., Olson, E.N., Arnold, H.H., and Wold, B.J. (1997). Different *MRF4* knockout alleles differentially disrupt Myf-5 expression: *cis*-regulatory interactions at the *MRF4/Myf-5* locus. Dev. Biol. *188*, 349–362.

Zhang, W., Behringer, R.R., and Olson, E.N. (1995). Inactivation of the myogenic bHLH gene *MRF4* results in up-regulation of myogenin and rib anomalies. Genes Dev. *9*, 1388–1399.